Thermal stability of $CoAu_{13}$ binary nanoparticle superlattices under the electron beam

Thermal Stability of $CoAu_{13}$ Binary Nanoparticle Superlattices under the Electron Beam

Thomas Altantzis,[a‡] Zhijie Yang,[b‡] Sara Bals,[a] Gustaaf Van Tendeloo,[a] Marie-Paule Pileni[c]*

[a] Electron Microscopy for Materials Research (EMAT), University of Antwerp, Groenenborgerlaan 171, 2020 Antwerp, Belgium

[b] Université Paris Diderot, Sorbonne Paris Cité, ITODYS, UMR 7086 CNRS, 15 Rue J-A de Baïf, 75205 Paris, Cedex 13, France

[c] CEA/IRAMIS, CEA Saclay F-91191 Gif-sur-Yvette, France

KEYWORDS: binary nanoparticle superlattices, electron beam, carbon deposition, stability, cobalt, gold

ABSTRACT: One primary goal of self-assembly in nanoscale regime is to implement multifunctional binary nanoparticle superlattices into practical use. In the last decade, considerable effort has been put into the fabrication of binary nanoparticle superlattices with controllable structure and stoichiometry. However, limited effort has been made in order to improve the stability of these binary nanoparticle superlattices, which is a prerequisite for their potential application. In this work, we demonstrate that the carbon deposition from specimen contamination can play an auxiliary role during the heat treatment of binary nanoparticle superlattices. With the in-situ carbon matrix formation, the thermal stability of $CoAu_{13}$ binary nanoparticle superlattices is unambiguously enhanced.

Wet chemistry synthetic methods now produce uniform nanoparticles of precisely controlled sizes, crystallinities and shapes.[1-3] These colloidal nanoparticles stabilized through steric interactions by a soft organic shell, provide a library of 'artificial atoms' that can be assembled into two-dimensional (2D) and three-dimensional (3D) nanoparticle superlattices, and which can be viewed as new type of solids.[4,5] The design of superlattices made of two different types of nanoparticles (A_xB_y), called binary nanoparticle superlattices, is becoming of particular importance because it provides a route to metamaterials with potentially new collective chemical or physical properties.[6-10] Numerous studies have been dedicated to the control of the crystalline structure of binary nanoparticle superlattices, composed of different types of nanomaterials (metals and/or semiconductors).[11-14] However, limited effort has been made in order to improve the stability of these binary nanoparticle superlattices, which is a prerequisite for their potential application.[15-17] It is well known that the melting point of metallic nanoparticles is remarkably reduced compared to that of their bulk counterpart and decreases further as the nanoparticle diameter becomes smaller.[18] The latter favors mass transfer between two nanoparticles in close contact despite their surface steric coatings. Binary superlattices stabilize smaller and less stable nanoparticles "B" embedded in the interstice of the larger and more stable nanoparticles "A". In other words, binary nanoparticle superlattices minimize the "B-B" contacts and consequently increase the stability of smaller nanoparticles. However, this effect does not take place for binary structures yielding "B-B" contacts, such as AB_4, AB_6, AB_{13} and quasicrystal structures. Improving the thermal stability of binary nanoparticle superlattices with "B-B" contacts remains challenging, since they tend to fuse together during thermal annealing.

By using aberration corrected High Angle Annular Dark-Field Scanning Transmission Electron Microscopy (HAADF-STEM), one is able to obtain atomic resolution images, in which the intensity depends on the atomic number of the elements present in the sample.[19] Here, we demonstrate that the carbon deposition from specimen contamination can play an auxiliary role during the heat treatment of binary nanoparticle superlattices.

Co and Au nanoparticles coated with oleic acid (C_{18}) and dodecanethiol (C_{12}) respectively, having low size distributions (<9%) were produced according to previous reports by using reverse micelles and hot-injection method, respectively (see Experimental Section in Supporting Information). Co and Au nanoparticles having a diameter of 7.2 and 3.7 nm respectively were used as large and small nanoparticles to achieve the rational co-crystallization (Figure S1, Supporting Information). 5.8×10^{-7} M of as-prepared Co nanoparticles were dispersed in toluene. The relative nanoparticle concentration was kept constant and equal to [Au]/[Co] = 10. A TEM image of the $NaZn_{13}$-type ($CoAu_{13}$) binary nanoparticle superlattice is presented in Figure 1a, oriented along a <100> axis. The corresponding Fast Fourier Transform (FFT) pattern, shown as inset in Figure 1a, yields a square symmetry and confirms the cubic lattice of the structure.[20] Note that both single component Au nanoparticle assemblies and AlB_2-type structures can be observed in some regions, which cannot be avoided during the formation of $NaZn_{13}$-type binary nanoparticle superlattices with a large excess of small nanoparticles (Figure 1b and Figure S2, Supporting Information). From the HAADF-STEM image (Figure 1c), it is clear that nanoparticles are highly ordered with formation of $CoAu_{13}$ superlattices. The brighter and darker features in the image correspond to Au (Z = 79) and Co (Z = 29) nanoparticles respectively. The Au nanoparticles are periodically ordered in a cubic framework whereas Co

nanoparticles are located at the centers of the Au cubic framework, creating a simple cubic lattice. To further verify these observations, Energy Dispersive X-ray spectroscopy in STEM mode (STEM-EDS) was performed at the area presented in Figure 1c. The resulting chemical maps are presented in Figure 1d-1f. The superposition of the two maps reveals a binary nanoparticle superlattice with $NaZn_{13}$ type structure, which is in agreement with the structural model, shown in Figure 1i.

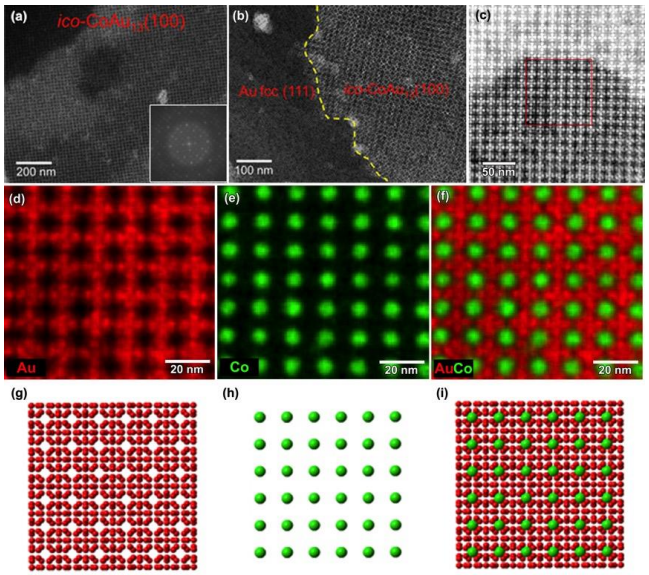

Figure 1. (a) TEM image of $NaZn_{13}$-type $CoAu_{13}$ binary nanoparticle superlattices. The FFT of the structure is given as an inset; (b) TEM image of the crystal boundary of single-component Au superlattices and $NaZn_{13}$-type $CoAu_{13}$ binary nanoparticle superlattices; (c) HAADF-STEM image of the $CoAu_{13}$ binary nanoparticle superlattice; (d-f) STEM-EDS elemental maps acquired from the region indicated by the red square in (c), where the distribution of the elements in the structure can be observed; (g-i) the corresponding crystal models.

The as-formed $CoAu_{13}$ sample was subjected to thermal annealing at 200°C for 5 min inside the TEM column, by using an in-situ heating holder. Three regions were investigated in-situ in STEM: Zones A, B corresponding to electron beam non-irradiated (A) and irradiated (B) $CoAu_{13}$ binary nanoparticle superlattices and zone C, corresponding to electron beam non-irradiated single component Au nanoparticle superlattice.

Zone A (without irradiation): The $CoAu_{13}$ binary nanoparticle superlattice can no longer be observed. The smaller 3.7-nm Au nanoparticles fuse into larger Au nanoparticles, whereas the 7.2-nm Co nanoparticles are stable against coalescence (Figure 2a and 2b). From the STEM-EDS analysis it can be concluded that the Co nanoparticles maintain their initial ordering into a simple cubic sub-lattice within the superlattice. The size of the Au nanoparticles evolved from 3.7 nm to 9.8 nm (see Figure S3, Supporting Information). Hence, in $CoAu_{13}$ binary nanoparticle superlattices, large Co nanoparticles form a simple cubic unit cell, which is filled with 13 Au nanoparticles, yielding an icosahedral nanoparticle cluster (Figure 2c). The HAADF-STEM images (Figure 3a) show that the fused Au particles are faceted. According to the theoretical prediction,[21] the 3.7-nm Au nanoparticles partially fused, forming in this way ad-atoms at the nanoparticles surfaces. A partial or total fusion of the Au nanoparticles takes place with the appearance of either inhomogeneous or highly homogeneous contrast. The presence of twinning in the Au nanoparticles after fusion (Figure 3b), reveals their polycrystallinity. Hence, by heating at 200 °C for 5 min, the structure of binary superlattices transits from $NaZn_{13}$-type $CoAu_{13}$ to CsCl-type CoAu with Co and Au nanoparticles sizes of 7.2 and 9.8 nm, respectively.

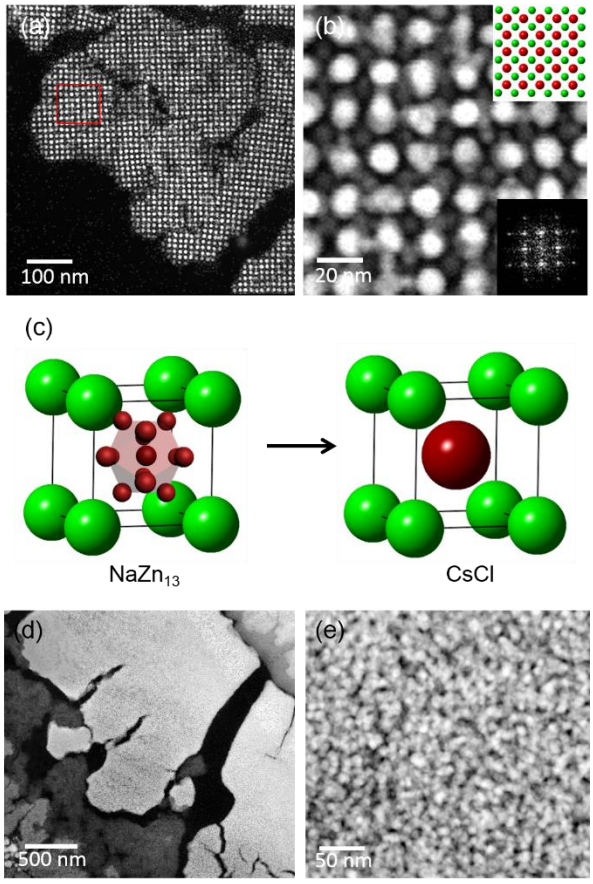

Figure 2. (a) HAADF-STEM image of non-irradiated $CoAu_{13}$ binary nanoparticle superlattices, heat treated in-situ in the TEM column at 200°C for 5 min; (b) magnified image of the region indicated by the red square in (a); (c) Schematic illustration of the structural transition from $NaZn_{13}$ to CsCl type binary nanoparticle superlattices; (d),(e) aggregation of the single component Au superlattices within the same sample.

Zone B ("*in situ*" e-beam irradiation): The influence of electron beam irradiation prior to in-situ thermal annealing on the stability of $CoAu_{13}$ binary superlattices was studied. The exposure time of the STEM observation is about 60s. The data remarkably differ from those observed without pre-irradiation treatment (Zone A). Figure 4a shows a brighter area within the square box, indicating that the deposition of carbonaceous materials on the surface of superlattices takes place after the electron beam irradiation. The carbon species on the sample surface are considered to be the main reason leading to the carbon layer deposition. As already mentioned, the nanoparticles used for growing binary superlattices are coated with long carbon chain surfactant (oleic acid and dodecanethiol). Upon high-energy electron beam irradiation, these organic molecules can be damaged and subjected to carbonization process.

After in-situ thermal annealing at 200°C for 5 min, the nanoparticles are still well ordered (Figure 4b), which is further confirmed by the corresponding FFT pattern (Figure 4c). The Au nanoparticles within the binary nanoparticle superlattice are well retained without any coalescence.

Zone C: As mentioned before, after deposited on TEM grid the mixture colloidal solution of Co and Au nanocrystals, the larger domain shows formation of $NaZn_{13}$-type superlattices whereas some regions show formation of 3.7-nm Au nanocrystals single component superlattices. Figures 1c and 2d-2e show the superlattices before and after e-beam irradiation respectively. The latter unambiguously reveals the occurrence of severe aggregations with formation of continuous wormlike structures.

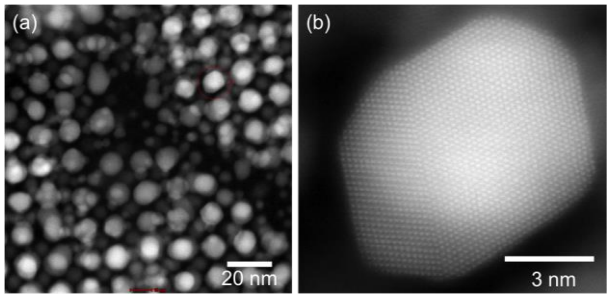

Figure 3. (a) High-magnification HAADF-STEM image of the Au nanoparticles within the CsCl-type binary nanoparticle superlattices; (b) high resolution HAADF-STEM image of the Au particle indicated by the red circle in (a). A twin defect is also present, revealing the polycrystallinity of the formed particles after fusion.

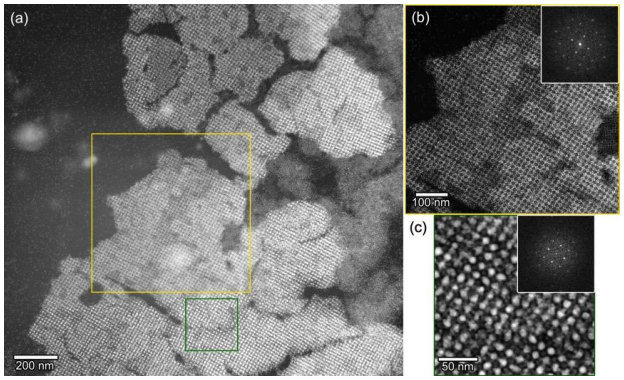

Figure 4. (a) Overview HAADF-STEM image of the $CoAu_{13}$ structure after heat treatment at 200°C for 5 min, where electron beam irradiated and non-irradiated regions are indicated with yellow and green squares respectively; (b) magnified image of the irradiated region in (a) with the FFT pattern shown as inset; (c) magnified image of the non-irradiated region in (a) with the FFT pattern shown as inset.

By comparing the results observed in Zones A and C, it can be concluded that Co arrays play the role of "scaffold", favoring the appearance of a new crystalline binary superlattice. Hence, the Co atoms at the nanoparticles surfaces can easily be oxidized into cobalt oxide, CoO.[22] This property enhances the nanoparticles stability against sintering.[23] As a result, Au nanoparticles within the binary nanoparticle superlattices sinter upon heat treatment, whereas Co nanoparticles remain stable. The un-sintered Co nanoparticle arrays serve as scaffold confining the sintering event of Au nanoparticles. Since the melting point of Au nanoparticles decreases with their size, adatoms freely diffusing in the "scaffold" appear. This favors the formation of either polycrystalline or coalesced nanoparticles as observed in Figure 3. Hence a new CsCl-type of binary crystal structure arises after heat treatment. This CsCl structure adopts a primitive cubic lattice with a two-atom basis. The Cl (Au) atoms are located at the vertices of a cubic unit cell, while the Cs (Co) atoms lie in the center of the cube (Figure 2c). Note that structural transformation from CaB6- to CsCl-type binary structures has been recently observed in Fe_2O_3/PbSe binary systems, where the fusion of six PbSe nanoparticles into one larger particle takes place.[17] The electron beam irradiation area is rather limited. So on a same TEM grid it is possible to observe region irradiated (Zone B) or not (Zone A). Hence, on the same image, a larger Au nanoparticle originated from the 13 small Au nanoparticles can be observed in square arrays, corresponding to a CsCl-type CoAu binary structure as described above (Figure 4b and 4c). After being embedded within a carbon layer, $CoAu_{13}$ binary nanoparticle superlattices show remarkable thermal stability against structure transformation from $NaZn_{13}$ to CsCl.

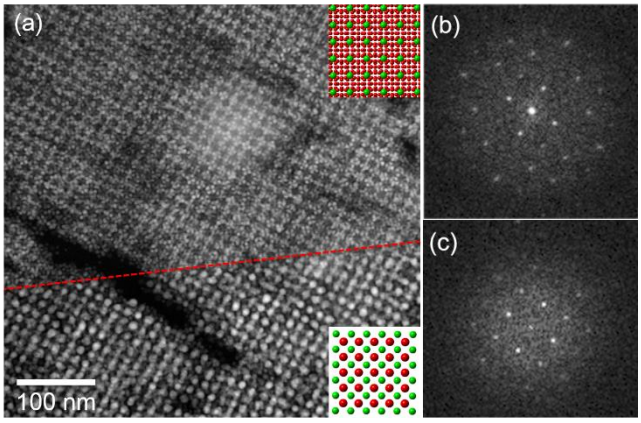

Figure 5. (a) Binary nanoparticle superlattices subjected to in-situ heat treatment at 200°C for 30 min; (b) and (c) are the corresponding FFT patterns from the upper and lower structures in (a); In (a), a clear crystal boundary can be found, indicated by the dashed red line.

This unexpected thermal stability was confirmed by extending the thermal treatment at 200 °C for 30 min. Figure 5 shows the HAADF-STEM image of the area after thermal treatment at 200°C for 30 min, and clearly exhibits the superlattice grain boundary. $NaZn_{13}$-type $CoAu_{13}$ and CsCl-type CoAu binary structure are abruptly separated without transition area. Both $CoAu_{13}$ and CoAu binary structures are highly stable after annealing. The thermal stability of CoAu binary structure can be attributed to the intrinsic crystal structure, where less-stable Au-Au contacts are not accessible and Au nanoparticles are isolated by the neighboring stable Co nanoparticles.

In summary, $NaZn_{13}$-type $CoAu_{13}$ binary nanoparticle superlattices have been produced. The thermal stability of those superlattices has been studied in-situ by STEM (Scheme S1, Supporting Information). Phase transformation from $NaZn_{13}$-type $CoAu_{13}$ to CsCl-type CoAu binary structure takes place through confined fusion of Au nanocrystals within a simple cubic Co nanoparticle array. Furthermore, unexpected high thermal stability of $CoAu_{13}$ binary nanoparticle superlattices was observed, after being embedded in a carbon matrix. This is achieved by in-situ electron beam irradiation. The carbon source of this carbon matrix mainly originates from the coat-

ing agent on the nanocrystals, and thus may produce a homogeneous carbon matrix. These findings may provide important insight into the application of binary nanoparticle superlattices.

ASSOCIATED CONTENT

Supporting Information. Experimental section, Figures S1-S3 and Scheme S1.This material is available free of charge via the Internet at http://pubs.acs.org.

AUTHOR INFORMATION

Corresponding Author

* To whom correspondence should be addressed. E-mail: mppileni@orange.fr

Author Contributions

‡These authors contributed equally.

Notes

The authors declare no competing financial interest.

ACKNOWLEDGMENT

The research leading to these results has been supported by an Advanced Grant of the European Research Council under Grant 267129. The authors appreciate financial support by the European Union under the Framework 7 program under a contract for an Integrated Infrastructure Initiative (Reference No.262348 ESMI). S.B. acknowledges funding from ERC Starting Grant COLOURATOMS (335078).

REFERENCES

(1) Peng, X. G.; Manna, L.; Yang, W. D.; Wickham, J.; Scher, E.; Kadavanich, A.; Alivisatos, A. P., Shape Control of Cdse Nanocrystals. *Nature* **2000,** *404*, 59-61.

(2) Yin, Y.; Alivisatos, A. P., Colloidal Nanocrystal Synthesis And The Organic-Inorganic Interface. *Nature* **2005,** *437*, 664-670.

(3) Pileni, M. P., The Role of Soft Colloidal Templates in Controlling The Size And Shape of Inorganic Nanocrystals. *Nat. Mater.* **2003,** *2*, 145-150.

(4) Murray, C. B.; Kagan, C. R.; Bawendi, M. G., Self-Organization Of Cdse Nanocrystallites into 3-Dimensional Quantum-Dot Superlattices. *Science* **1995,** *270*, 1335-1338.

(5) Pileni, M. P., Nanocrystal Self-Assemblies: Fabrication And Collective Properties. *J. Phys. Chem. B* **2001,** *105*, 3358-3371.

(6) Kalsin, A. M.; Fialkowski, M.; Paszewski, M.; Smoukov, S. K.; Bishop, K. J. M.; Grzybowski, B. A., Electrostatic Self-Assembly Of Binary Nanoparticle Crystals With A Diamond-Like Lattice. *Science* **2006,** *312*, 420-424.

(7) Shevchenko, E. V.; Talapin, D. V.; Kotov, N. A.; O'Brien, S.; Murray, C. B., Structural Diversity in Binary Nanoparticle Superlattices. *Nature* **2006,** *439*, 55-59.

(8) Dong, A. G.; Chen, J.; Vora, P. M.; Kikkawa, J. M.; Murray, C. B., Binary Nanocrystal Superlattice Membranes Self-Assembled at The Liquid-Air Interface. *Nature* **2010,** *466*, 474-477.

(9) Sun, Z.; Luo, Z.; Fang, J., Assembling Nonspherical 2D Binary Nanoparticle Superlattices By Opposite Electrical Charges: The Role of Coulomb Forces. *ACS Nano* **2010,** *4*, 1821-1828.

(10) Smith, D. K.; Goodfellow, B.; Smilgies, D. M.; Korgel, B. A., Self-Assembled Simple Hexagonal AB(2) Binary Nanocrystal Superlattices: SEM, GISAXS, And Defects. *J. Am. Chem. Soc.* **2009,** *131*, 3281-3290.

(11) Bodnarchuk, M. I.; Kovalenko, M. V.; Heiss, W.; Talapin, D. V., Energetic And Entropic Contributions To Self-Assembly Of Binary Nanocrystal Superlattices: Temperature As The Structure-Directing Factor. *J. Am. Chem. Soc.* **2010,** *132*, 11967-11977.

(12) Yang, Z.; Wei, J.; Bonville, P.; Pileni, M.-P., Beyond Entropy: Magnetic Forces Induce Formation Of Quasicrystalline Structure In Binary Nanocrystal Superlattices. *J. Am. Chem. Soc.* **2015,** *137*, 4487-4493.

(13) Evers, W. H.; Nijs, B. D.; Filion, L.; Castillo, S.; Dijkstra, M.; Vanmaekelbergh, D., Entropy-Driven Formation of Binary Semiconductor-Nanocrystal Superlattices. *Nano Lett.* **2010,** *10*, 4235-4241.

(14) Yang, Z.; Wei, J.; Pileni, M.-P., Metal-Metal Binary Nanoparticle Superlattices: A Case Study of Mixing Co And Ag Nanoparticles. *Chem. Mater.* **2015,** *27*, 2152-2157.

(15) Kang, Y.; Ye, X.; Chen, J.; Qi, L.; Diaz, R. E.; Doan-Nguyen, V.; Xing, G.; Kagan, C. R.; Li, J.; Gorte, R. J.; Stach, E. A.; Murray, C. B., Engineering Catalytic Contacts And Thermal Stability: Gold/Iron Oxide Binary Nanocrystal Superlattices For CO Oxidation. *J. Am. Chem. Soc.* **2013,** *135*, 1499-1505.

(16) Yu, Y.; Bosoy, C. A.; Smilgies, D.-M.; Korgel, B. A., Self-Assembly And Thermal Stability Of Binary Superlattices Of Gold And Silicon Nanocrystals. *J. Phys. Chem. Lett.* **2013,** *4*, 3677-3682.

(17) Treml, B. E.; Lukose, B.; Clancy, P.; Smilgies, D.-M.; Hanrath, T., Connecting The Particles In The Box - Controlled Fusion Of Hexamer Nanocrystal Clusters Within An AB_6 Binary Nanocrystal Superlattice. *Sci. Rep.* **2014,** *4*. 6731.

(18) Buffat, P.; Borel, J. P., Size Effect On The Melting Temperature Of Gold Particles. *Phys. Rev. A* **1976,** *13*, 2287-2298.

(19) Browning, N. D.; Chisholm, M. F.; Pennycook, S. J., Atomic-Resolution Chemical Analysis Using A Scanning Transmission Electron Microscope. *Nature* **1993,** *366*, 143-146.

(20) Chen, J.; Ye, X.; Murray, C. B., Systematic Electron Crystallographic Studies of Self-Assembled Binary Nanocrystal Superlattices. *ACS Nano* **2010,** *4*, 2374-2381.

(21) Shim, J. H.; Lee, B. J.; Cho, Y. W. Thermal Stability of Unsupported Gold Nanoparticle: A Molecular Dynamics Study. *Surf. Sci.* **2002,** *512*, 262–268.

(22) Yang, Z. J.; Yang, N. L.; Pileni, M. P. Nano Kirkendall Effect Related to Nanocrystallinity of Metal Nanocrystals: Influence of the Outward and Inward Atomic Diffusion on the Final Nanoparticle Structure. *J. Phys. Chem. C* **2015,** *119*, 22249-22260.

(23) Cabrera, N.; Mott, N. F., Theory of The Oxidation Of Metals. *Rep. Progress Phys.* **1948,** *12*, 163-184.